Processing and Application of Ceramics 18 [3] (2024) 314–322
https://doi.org/10.2298/PAC2403314C

Phase relations in the Nd_2O_3-Fe_2O_3 system: Structure and magnetic properties of perovskite $NdFeO_3$ ceramics

Olga V. Chudinovych[1,2,*], Dmytro V. Vedel[1], Oleksandr O. Stasyuk[3], Anatoly V. Samelyuk[1], Myriam H. Aguirre[4,5,6]

[1]*I.M. Frantsevich Institute for Problems in Materials Science NAS of Ukraine, 3, Omeliana Pritsaka St., 03142, Kyiv, Ukraine*
[2]*National Technical University of Ukraine - Igor Sikorsky Kyiv Polytechnic Institute, 37, Peremohy Ave., 03056, Kyiv, Ukraine*
[3]*G.V. Kurdyumov Institute for Metal Physics of the NAS of Ukraine, 36, Akademika Vernadskyi Boulev., 02000, Kyiv, Ukraine*
[4]*Institute of Nanoscience and Materials of Aragon, University of Zaragoza-CSIC, Mariano Esquillor s/n, 50018, Zaragoza, Spain*
[5]*Department of Physics Condensed Matter, University of Zaragoza, Pedro Cerbuna 12, Zaragoza, Spain*
[6]*Laboratory of Advanced Microscopy, University of Zaragoza, Mariano Esquillor s/n, 50018, Zaragoza, Spain*

Received 24 July 2024; Received in revised form 14 September 2024; Accepted 19 September 2024

Abstract

The phase relations in the Nd_2O_3-Fe_2O_3 system at 1300 and 1400 °C were studied in the whole concentration range by X-ray diffraction (XRD) and scanning electron microscopy (SEM). The isothermal cross-sections of the Nd_2O_3-Fe_2O_3 phase diagram at 1300 and 1400 °C are characterized by the presence of three single-phase (A-Nd_2O_3, $NdFeO_3$, Fe_2O_3) and two two-phase (A-Nd_2O_3 + $NdFeO_3$, $NdFeO_3$ + Fe_2O_3) regions. The composition corresponding to the perovskite phase is 51 mol% Nd_2O_3 – 49 mol% Fe_2O_3. In the next step, the investigation was focused on this composition. Nanocrystalline $NdFeO_3$ powders with perovskite structure were obtained by the Pechini method and heterogeneous precipitation from nitrate solutions. The influence of the production method on the microstructure, morphology and magnetic properties of the $NdFeO_3$ nanopowders was studied. According to XRD, SEM and TEM, the synthesized perovskite $NdFeO_3$ is single-phase with a particle size of 60–90 nm. The morphology of powder particles primarily depends on the synthesis method. The powder showed ferromagnetic behaviour and had saturation magnetization 0.8 and 0.81 emu/g.

Keywords: *Nd_2O_3-Fe_2O_3 system, phase relations, perovskite-type $NdFeO_3$ phase, magnetic properties*

I. Introduction

Currently, various types of dielectric, magnetic and magnetodielectric materials are widely studied. Nanoscale dielectric materials such as SiO_2, ZnO and BN exhibit excellent electromagnetic absorption characteristics in the high-frequency range [1]. On the other hand, magnetic materials such as Fe_3O_4, $BaTiO_3$ and $BaFe_{12}O_{19}$ exhibit high absorption characteristics in various frequency ranges [1]. However, their use is limited by a high tendency to demagnetization. Therefore, much attention is currently focused on synthesizing magnetic materials with better magnetic and dielectric properties.

Rare earth perovskite orthoferrites ($RFeO_3$) have attracted considerable attention due to their physicochemical characteristics, which include magnetic phenomena and magneto-optical effects, resulting from complex interactions between two different magnetic sublattices of R^{3+} and Fe^{3+} [1,2]. The crystal structure of $RFeO_3$ is simple and stable, and most metal elements can be dissolved in the perovskite lattice [1]. $RFeO_3$ typically consists of rare earth elements with large ionic radii in the

* Corresponding author: tel: +380977130309
e-mail: *chudinovych_olia@ukr.net*

A-position and transition metals with small ionic radii in the B-position. The Fe atom is located in the centre surrounded by six O atoms, forming the octahedral structure FeO_6, while the R atom is located in the position made from these octahedra bonded to twelve O atoms [1]. Different ionic radii of R^{3+} and Fe^{3+} affect the FeO_6 octahedron, change the length of Fe–O bonds and Fe–O–Fe bond angle, and distort the structure, thereby affecting the properties [1]. Due to the combination of magnetic and dielectric properties, perovskite ferrite materials have a wide range of applications: radio engineering, electronics, computer technology, catalysis, gas-separating fuel cells, magneto-optical devices, electromagnetic equipment, environmental monitoring, gas sensors, solid oxide fuel cells, photocatalysis etc. [1–7].

$NdFeO_3$ is a typical orthoferrite and its magnetic properties mainly depend on the interactions between Nd^{3+}–Fe^{3+}, Fe^{3+}–Fe^{3+} and Nd^{3+}–Nd^{3+} [2]. The coexistence of such interactions in orthoferrites provides physical properties such as magnetoelectric effects, spin Hall magnetoresistance and spin Seebeck effect [5]. $NdFeO_3$ is prepared by various methods: sol-gel method [2,8–13], solid state reaction [14,15] and hydrothermal method [16]. It should be noted that the chemical composition of the components obtained by these synthesis techniques was not systematically investigated [2,8–16].

The right choice of optimal compositions for the synthesis of materials is the key to obtaining materials with the desired physical and chemical properties. The reference material for determining the optimal compositions is the phase diagram, as it can be used to determine the region of existence of solid solutions. The phase diagram of Fe_2O_3-Nd_2O_3 has been studied by various scientists, but the data contradict each other and need to be clarified [17–20]. Thus, Jakobsson *et al.* [17] investigated thermal behaviour in the FeO-Fe_2O_3-Nd_2O_3 system, but a small number of experimental samples were taken. In addition, the calculated thermodynamic characteristics of various lanthanide orthoferrites were analysed [18–20], but there is a lack of systematism in the obtained results. All this indicates the need for a systematic study of the phase equilibria in this system and the determination of the composition corresponding to the perovskite-type phase.

This work aims to study the interaction of neodymium and iron oxides at 1300 and 1400 °C in the whole concentration range, and determine the composition range where the single phase $NdFeO_3$ perovskite is stable. In addition, the perovskite-type $NdFeO_3$ powders were synthesized by Pechini and heterogeneous precipitation methods and their structure and magnetic properties were investigated.

II. Experimental

Nd_2O_3 with purity of 99.99% (purchased from Merck Corp.), $Fe(NO_3)_3 \cdot 9\,H_2O$ (purchased from Merck Corp.), ammonia, NH_2CONH_2 and nitric acid were used as starting materials. The specimens with different concentrations of Fe_2O_3 ($x$$Nd_2O_3$–(100-$x$)$Fe_2O_3$ where x corresponds to 0, 0.5, 1, 2, 5, 15, 30, 45, 49, 50, 51, 55, 85, 90, 95 and 100 mol%) were prepared from Nd^{3+}/Fe^{3+} nitrate solutions with their subsequent evaporation and decomposition at 800 °C for 2 h. Solutions of Nd^{3+} nitrate were obtained by dissolving neodymium oxide in nitric acid. Before preparing the initial solutions, neodymium oxide was pre-dried in a muffle furnace at 300 °C for 2 h. The prepared Nd_2O_3-Fe_2O_3 powders were pressed at 10 MPa into pellets of 5 mm in diameter and 4 mm in height. To study phase relationships at 1300 and 1400 °C thermal treatment of the as-prepared samples was carried out in two stages: at 1100 °C (for 100 h in air) and then at 1300 °C (for 300 h in air) and 1400 °C (for 100 h in air) in the furnaces with heating elements based on Fecral (H23U5T) and Superkanthal ($MoSi_2$), respectively. The heating rate was 3 °C/min.

Nanopowders with selected composition, enabling synthesis of the perovskite phase, were obtained by the Pechini method ($NdFeO_3$(I)) and heterogeneous precipitation ($NdFeO_3$(II)). The essence of the Pechini method is to achieve a high degree of cations mixing in the solution, the controlled transition of the solution into a polymer gel, the removal of the polymer matrix with the formation of an oxide precursor, and the preservation of a high degree of homogeneity. A mixture with different Nd^{3+} and Fe^{3+} content was prepared from nitrate solutions (Nd^{3+} nitrate solutions were obtained from Nd_2O_3). The mixture of nitrates and citric acid solutions was stirred for 1 h at 80 °C. The obtained precursor was dried at 150 °C for 24 h and then subjected to heat treatment at 800 °C.

The $NdFeO_3$(II) precursor was synthesized by the method of heterogeneous precipitation from a mixture of Nd^{3+} and Fe^{3+} nitrate solutions at a concentration of 0.1 mol/l at 80 °C. As a precipitant, the 1 M ammonia solution with a 5 vol.% urea was used. The obtained precipitated particles were separated by triple centrifugation with distilled water and a single centrifugation in the presence of ethyl alcohol and dried at 120 °C for 24 h.

The sample characterization was carried out using physicochemical methods: X-ray diffraction (XRD), thermogravimetric analysis and electron microscopy (SEM, TEM). For phase composition analysis, X-ray patterns were obtained on the X-ray diffractometer DRON-3M (CuKα radiation with a nickel filter). The scan angle step was 0.05–0.1° in the range 2θ = 15–80°. A DQ-1000 instrument was used for thermogravimetric analysis. Scanning electron microscopy (SEM) was used to assess the homogeneity of the powders. Elemental analysis of the samples was performed by X-ray spectral microanalysis (XMR) using an energy dispersive spectrometer (EDS) INCA 450, OXFORD Instruments). Transmission electron microscopy (TEM) was performed by Tecnai F30 (FEI) working at 300 keV

with EDS *in situ* spectroscopy. The atomic concentrations of the elements were determined within the relative experimental error of ~0.2% for the investigated area of 500 μm × 500 μm. The specimens with dimensions 5 mm in diameter and 2 mm in height and powders were used to measure magnetic properties. A cuvette measurement of magnetic properties was performed on the vibrating sample magnetometer (LDJ-9500, LDJ Electronics, Troy, MI 48099, USA) by using magnetostatic measurement that creates a working acceleration of 25 gn, where gn is the standard gravity. The determined magnetization (M) in function of magnetic field (H) of the samples in the magnetic field range between −10 and +10 kOe were completely reproducible after repeated recording at room temperature.

III. Results and discussion

3.1. Phase composition in Nd_2O_3–Fe_2O_3 system

The chemical and phase compositions in Nd_2O_3–Fe_2O_3 system annealed at 1300 and 1400 °C with lattice parameter data are summarized in Tables 1 and 2, respectively. The results were used to plot the isothermal section of the Nd_2O_3–Fe_2O_3 phase diagram at 1300 and 1400 °C (Fig. 1).

There are Nd_2O_3, Fe_2O_3 and $NdFeO_3$ (R) phases in Nd_2O_3–Fe_2O_3 system at 1300 and 1400 °C, according to XRD and SEM analyses, Figs. 2-4. Note that the neodymium oxide in air undergoes hydration and thus, instead of hexagonal Nd_2O_3 phase in the samples at 1300 and 1400 °C we found the formation of hexagonal hydroxide of $Nd(OH)_3$ (Fig. 3d,e). Nevertheless, since this applies only to Nd_2O_3 in the investigated system, the results obtained for $Nd(OH)_3$ can be attributed to A-Nd_2O_3.

$NdFeO_3$ does not form regions of homogeneity, but only the specific composition corresponding to 51 mol% Nd_2O_3 – 49 mol% Fe_2O_3 at which it exists (Fig. 1, Tables 1 and 2). A change of the composition by just 1 mol% leads to a shift from a single-phase region ($NdFeO_3$) to a two-phase region ($NdFeO_3$ + Nd_2O_3 and $NdFeO_3$ + Fe_2O_3). The pure Fe_2O_3 and Nd_2O_3 phases also do not form regions of homogeneity (Fig. 1, Tables 1 and 2).

In the system Nd_2O_3–Fe_2O_3 at 1300 and 1400 °C, the ordered phase of perovskite type with rhombic distortion has been revealed. The composition corresponding to the perovskite phase (labelled as R) is 51 mol% Nd_2O_3 – 49 mol% Fe_2O_3. The lattice parameters of the unit cell of R-phase vary from a = 0.587 nm, b = 0.775 nm, c = 0.544 nm in the single-phase sample containing 51 mol% Nd_2O_3 – 49 mol% Fe_2O_3 to a = 0.558 nm, b = 0.777 nm, c = 0.534 nm in the two-phase sample (A + R), containing 70 mol% Nd_2O_3 – 30 mol% Fe_2O_3 and to a = 0.558 nm, b = 0.777 nm, c =

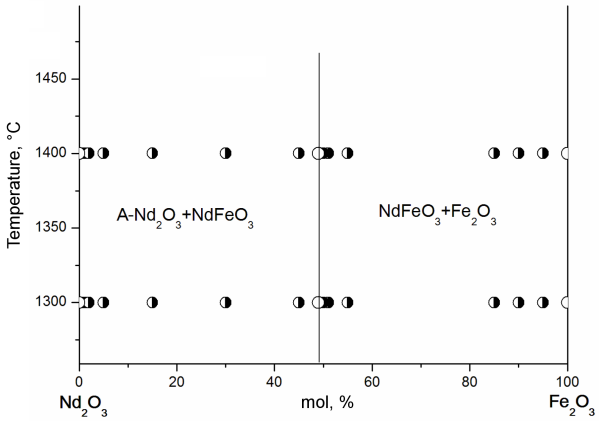

Figure 1. Isothermal sections at 1300 and 1400 °C for the system Nd_2O_3–Fe_2O_3 (○ – single-phase samples, ◑ – two-phase samples)

Table 1. Phase composition and lattice parameters in the Nd_2O_3–Fe_2O_3 system annealed at 1300 °C for 300 h in air (XRD and SEM data)

Composition [mol%]		Phases by XRD	Lattice parameters of the phases, σ ± 0.0002 [nm]						
			R			Fe_2O_3		$Nd(OH)_3$	
Fe_2O_3	Nd_2O_3		a	b	c	a	c	a	c
100	0	Fe_2O_3				0.511	1.382		
95	5	Fe_2O_3 + R	0.556	0.776	0.544	0.509	1.373		
90	10	Fe_2O_3 + R	0.559	0.773	0.545	0.506	1.373		
85	15	Fe_2O_3 + R	0.557	0.774	0.545	0.509	1.373		
55	45	Fe_2O_3 + R	0.561	0.770	0.545	0.507	1.367		
51	49	Fe_2O_3 + R	0.557	0.776	0.542	0.505	1.377		
50	50	Fe_2O_3 + R	0.558	0.777	0.545				
49	51	R	0.587	0.775	0.544				
45	55	R + $Nd(OH)_3$	0.558	0.777	0.546				
30	70	R + $Nd(OH)_3$	0.558	0.777	0.534			0.632	0.375
15	85	R + $Nd(OH)_3$	0.570	0.775	0.542			0.638	0.373
5	95	R + $Nd(OH)_3$	0.557	0.800	0.541			0.639	0.377
2	98	R + $Nd(OH)_3$						0.643	0.367
1	99	R + $Nd(OH)_3$						0.643	0.372
0.5	99.5	R + $Nd(OH)_3$						0.642	0.371
0	100	$Nd(OH)_3$						0.642	0.374

Table 2. Phase composition and lattice parameters in the Nd_2O_3–Fe_2O_3 system, annealed at 1400 °C for 100 h in air (XRD and SEM data)

Composition [mol%]		Phases by XRD	Lattice parameters of the phases, $\sigma \pm 0.0002$ [nm]						
			R			Fe_2O_3		$Nd(OH)_3$	
Fe_2O_3	Nd_2O_3		*a*	*b*	*c*	*a*	*c*	*a*	*c*
100	0	Fe_2O_3				0.511	1.382		
95	5	Fe_2O_3 + R				0.509	1.370		
90	10	Fe_2O_3 + R	0.558	0.762	0.548	0.503	1.374		
85	15	Fe_2O_3 + R	0.556	0.777	0.537	0.509	1.374		
55	45	Fe_2O_3 + R	0.559	0.779	0.530				
51	49	Fe_2O_3 + R	0.558	0.779	0.531				
50	50	Fe_2O_3 + R	0.558	0.775	0.539				
49	51	R	0.683	0.741	0.510				
45	55	R + $Nd(OH)_3$	0.558	0.777	0.539				
30	70	R + $Nd(OH)_3$	0.557	0.766	0.549			0.643	0.372
15	85	R + $Nd(OH)_3$	0.562	0.808	0.503			0.644	0.370
5	95	R + $Nd(OH)_3$						0.643	0.373
2	98	R + $Nd(OH)_3$						0.642	0.373
1	99	R + $Nd(OH)_3$						0.641	0.372
0.5	99.5	R + $Nd(OH)_3$						0.642	0.372
0	100	$Nd(OH)_3$						0.642	0.374

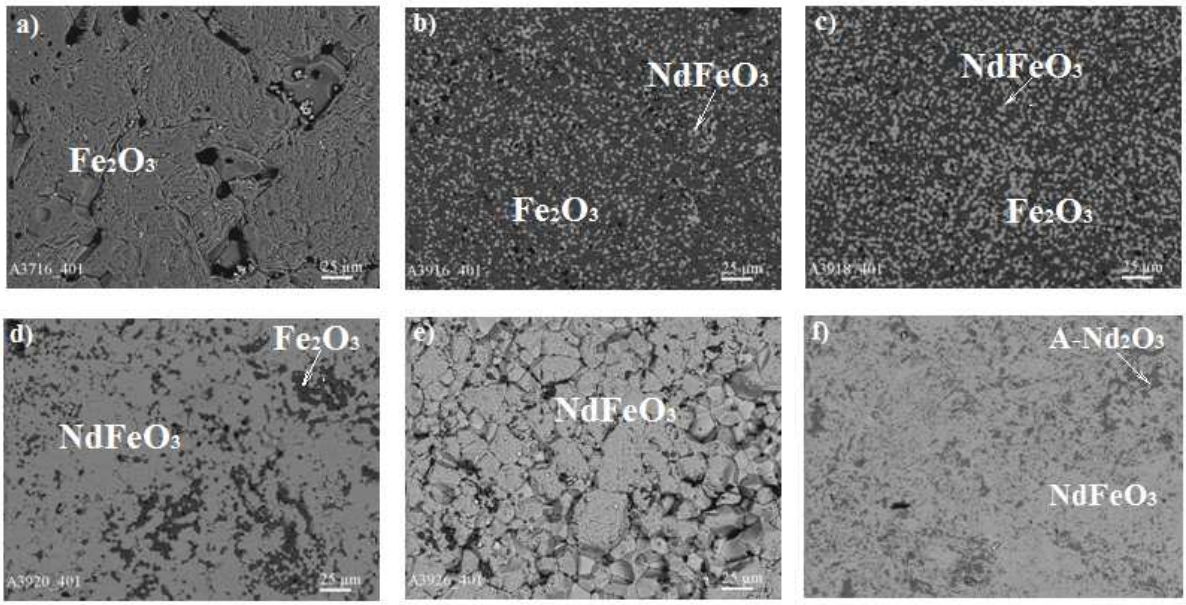

Figure 2. SEM microstructures of the samples heat-treated at 1300 °C: a) $0Nd_2O_3$–$100Fe_2O_3$, b) $5Nd_2O_3$–$95Fe_2O_3$, c) $10Nd_2O_3$–$90Fe_2O_3$, d) $15Nd_2O_3$–$85Fe_2O_3$, e) $51Nd_2O_3$–$49Fe_2O_3$ and f) $55Nd_2O_3$–$45Fe_2O_3$

0.546 nm in the two-phase sample (R + Fe_2O_3), containing 50 mol% Nd_2O_3 – 50 mol% Fe_2O_3 heat-treated at 1300 °C (Fig. 5). The EDS spectra for $NdFeO_3$ confirm the presence of three elements: Nd, Fe and O (Fig. 6).

3.2. Structure of perovskite $NdFeO_3$ powders

DTA curves of the precursor $NdFeO_3$ powders obtained by the Pechini method and heterogeneous precipitation illustrate the presence of minima. Above 680 °C, no thermal effects are recorded, and there is no mass loss in the sample. The endothermic peaks on the DTA curves in the low-temperature region are associated with the removal of adsorbed and structurally bound water and the decomposition of intermediate compounds. An intense endothermic effect at 640 °C corresponds to the crystallization of the final product (Fig. 7a). Each effect of the DTA curve corresponds to the loss of mass on the TG curve. The total mass losses of both samples were ~69 % (Fig. 7a) and ~36 % (Fig. 7b). The decomposition process of the synthesized precursors completed at ~800 °C, depending on their synthesis, phase composition, amorphous or amorphous crystalline state, specific surface area and primary size of mesopores. The absence of extremes from 670 to 1000 °C indicates that the reaction is complete and no phase transitions occur in the sample.

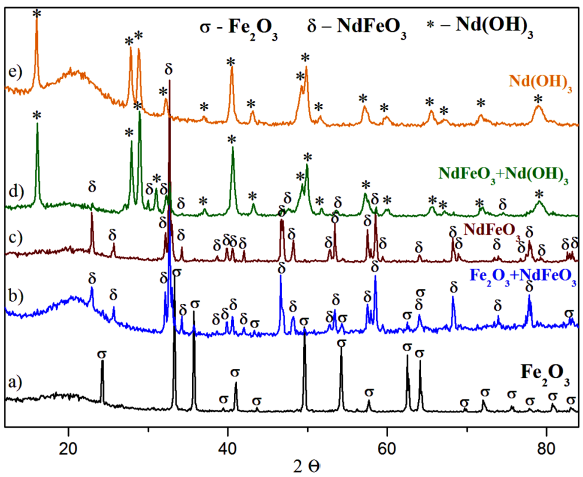

Figure 3. Isothermal sections at 1300 and 1400 °C for the system Nd_2O_3–Fe_2O_3 (○ – single-phase samples, ◑ – two-phase samples)

Figure 8 presents XRD of the powders obtained by two different methods. The precursors are amorphous because they have a broad, blurred peak (halo) at 18–28°. Only one phase is present in all samples heat-treated at 800 °C. The presence of other peaks corresponding to Nd, Nd_2O_3, Fe_2O_3, or any additional phases was not observed. The detected main peaks belong to the planes (020), (111), (200), (121), (210), (220), (022), (131), (122), (040), (212), (044), (311), (240), (123), (410) and (204).

Table 3. Structural properties of nanopowders based on the perovskite phase

Samples	Unit cell parameters [nm]			V [nm^3]
	a	*b*	*c*	
$NdFeO_3$(I)	0.5620	0.7649	0.5444	0.2340
$NdFeO_3$(II)	0.5720	0.7744	0.5445	0.2412

The EDS spectra of NdFeO3(I) and NdFeO3(II) synthesized by the two methods have three elements: Nd, Fe and O. Contents of Nd were 22.83 and 23.75 at.% and for Fe were 22.79 and 23.06 at.% in the $NdFeO_3$(I) and $NdFeO_3$(II), respectively. Regardless of the preparation technology, the powders had an agglomerated form (Figs. 9a and 10a). A more detailed analysis at high magnifications revealed particles whose size does not exceed 100 nm (Figs. 9b and 10b). The morphology of the powder particles primarily depends on the method of material synthesis. Larger particles consist of several nuclei with internal boundaries between them that were formed in competition between the processes of nucleation and growth of nuclei.

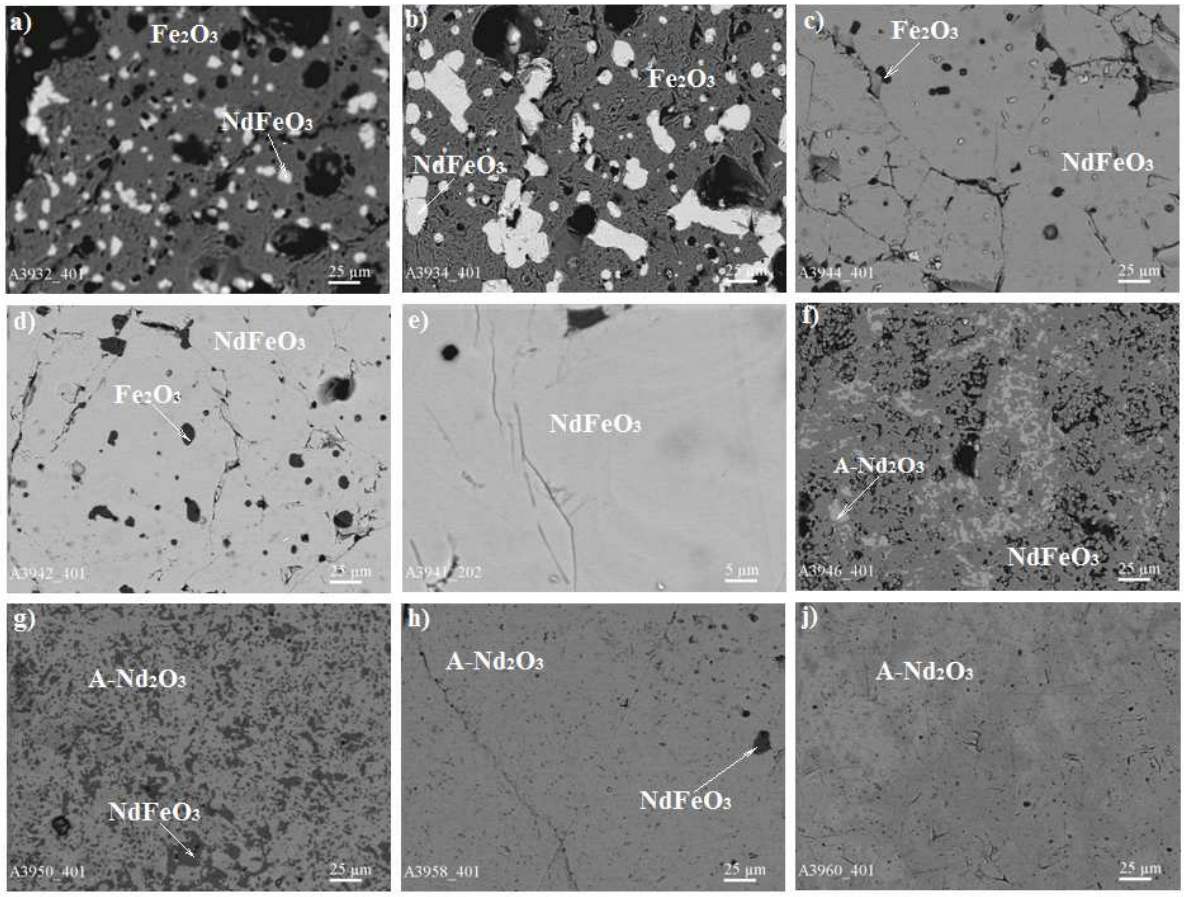

Figure 4. SEM microstructures of the samples heat-treated at 1400 °C: a) $5Nd_2O_3$–$95Fe_2O_3$, b) $10Nd_2O_3$–$90Fe_2O_3$, c) $49Nd_2O_3$–$51Fe_2O_3$, d) $50Nd_2O_3$–$50Fe_2O_3$, e) $51Nd_2O_3$–$49Fe_2O_3$, f) $55Nd_2O_3$–$45Fe_2O_3$, g) $85Nd_2O_3$–$15Fe_2O_3$, h) $99.5Nd_2O_3$–$0.5Fe_2O_3$ and j) $100Nd_2O_3$–$0Fe_2O_3$

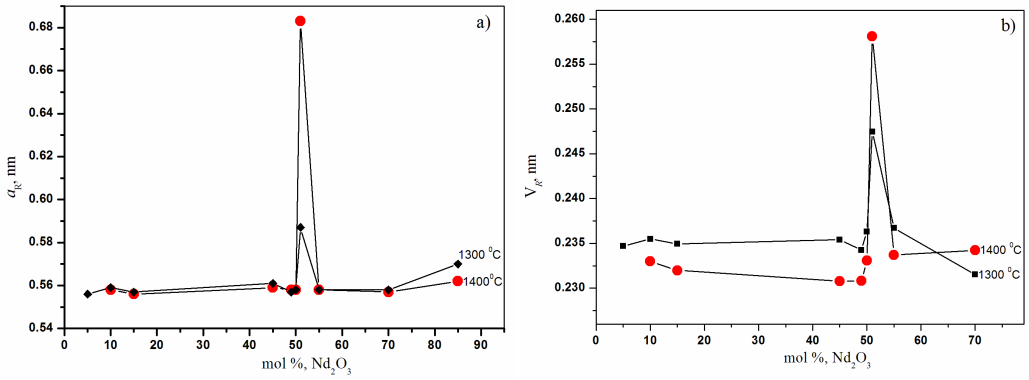

Figure 5. Concentration dependence of lattice parameters of R-phase ($NdFeO_3$) (a) and volume of elementary cell for R-phase (b) versus neodymia concentration

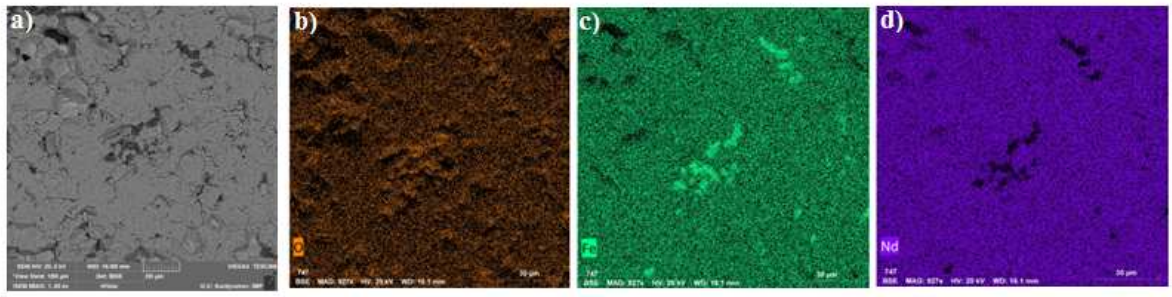

Figure 6. Microphotograph of $NdFeO_3$ (a) particle with EDS mapping for: oxygen (b), iron (c) and neodymium (d)

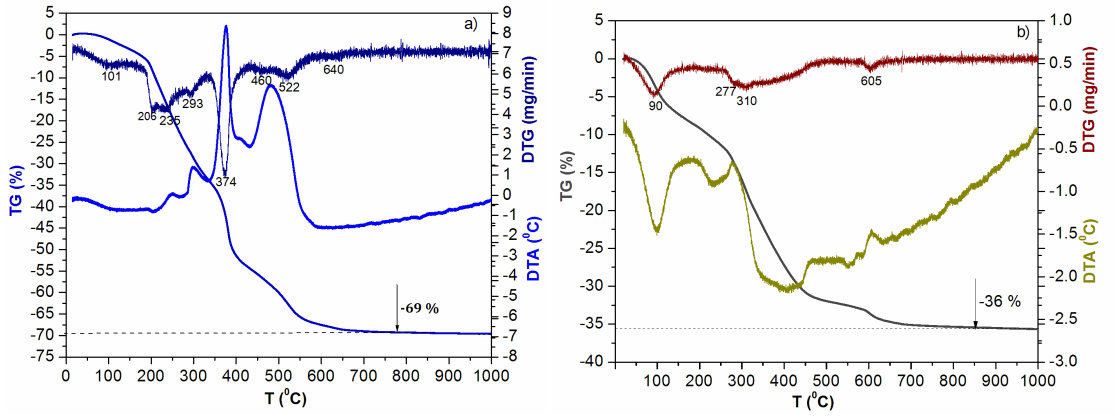

Figure 7. Thermal analysis curves of precursor powders: a) Pechini method (I), b) heterogeneous precipitation method (II)

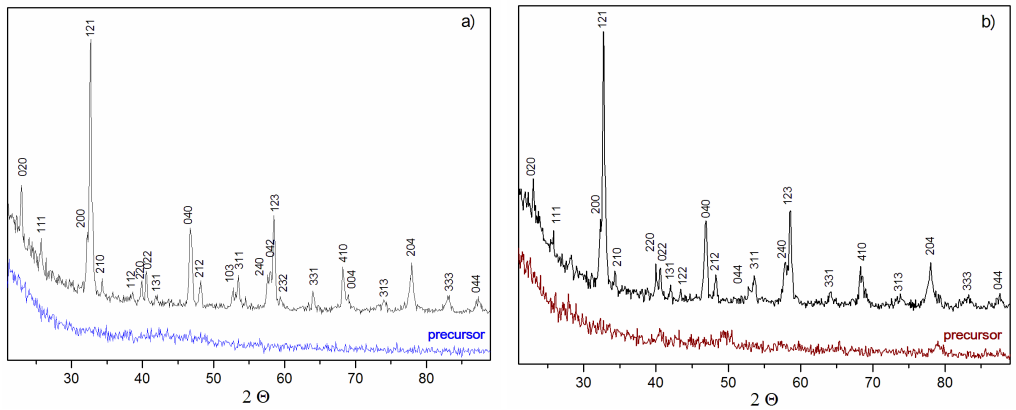

Figure 8. XRD of nanopowders (precursor and calcined at 800 °C) based on the perovskite phase: a) Pechini method (I), b) heterogeneous precipitation method (II)

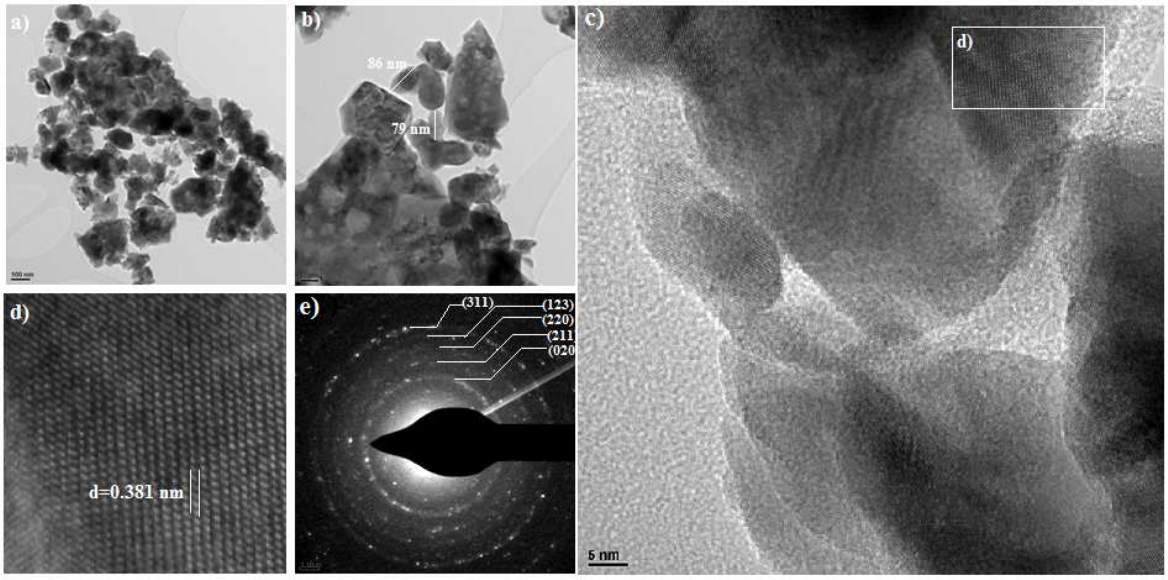

Figure 9. TEM of $NdFeO_3$ synthesized by I method and calcined at 800 °C: (a-c,e) and SAED of particles (d)

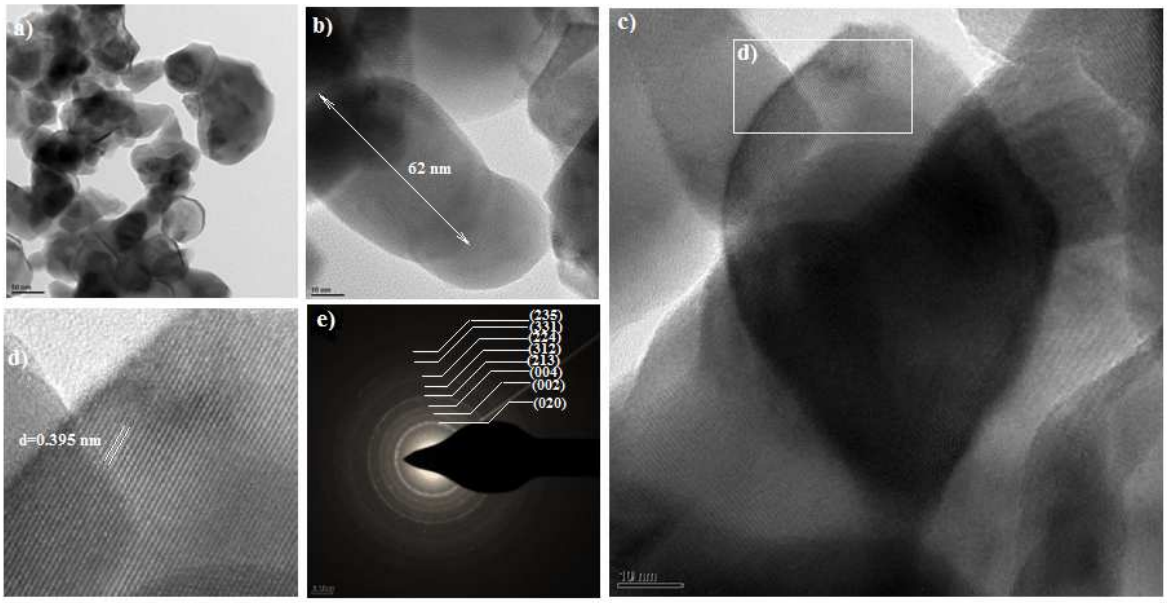

Figure 10. TEM of $NdFeO_3$ synthesized by II method and calcined at 800 °C: (a-c,e) and SAED of particles (d)

The electron diffraction pattern (SAED) of the polycrystalline $NdFeO_3$ is fully consistent with the theoretical calculation with the presence of all diffraction reflections (Figs. 9d and 10d). The HRTEM images (Figs. 9e and 10e) confirm high crystallinity and show clear interplanar spacings of d = 0.381 and 0.395 nm, which correspond to the crystallographic planes (002) and (111) of $NdFeO_3$, respectively.

Thus, the synthesized materials fully corresponded to the $NdFeO_3$ phase both in terms of chemical analysis and diffraction. The Pechini method produces more agglomerated particles, which leads to a diffraction pattern similar to that of a polycrystalline material. At the same time, synthesis by heterogeneous precipitation produces more homogeneous and less agglomerated particles.

3.3. Magnetic properties of $NdFeO_3$ powders

The H vs. M curves of the materials synthesized by using different methods and at 1300 °C are depicted in Figs. 11 and 12.

The materials obtained at temperature of 1300 °C have a dense non-porous structure. Dense materials had domains and could be magnetized in the strong magnetic field. It should be emphasized that those magnetic properties, like M and coercivity, are approximately the same for the $NdFeO_3$(I) and $NdFeO_3$(II) samples. This was because the dense microstructure was formed and the synthesis method has low influence.

The bulk $NdFeO_3$ was found to possess long-range antiferromagnetic (AFM) order below the Néel temperature. The crystal-field spectrum of the Nd^{3+} ions spans

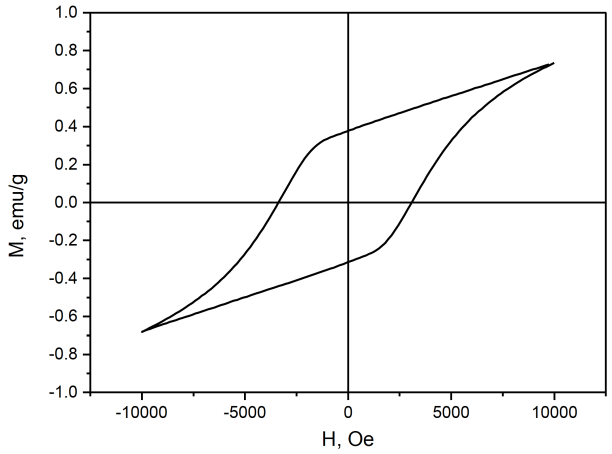

Figure 11. Magnetic properties of $NdFeO_3$ (I) synthesized at 1300 °C

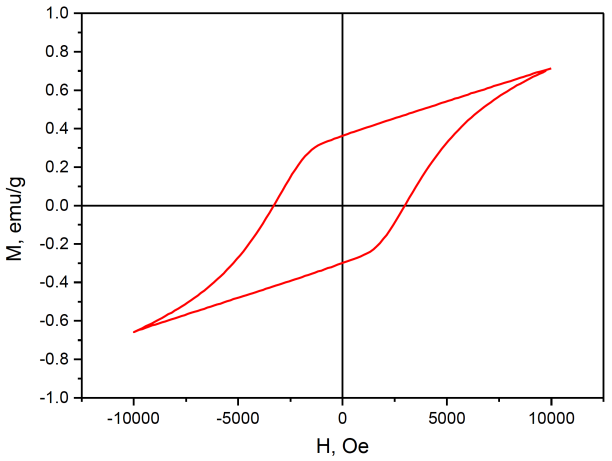

Figure 12. Magnetic properties of $NdFeO_3$ (II) synthesized at 1300 °C

an energy range between 3 and 60 meV; in zero field the XY-like spins are in the *ab* plane with a magnetic moment of 1.89(5) μB/ion [24].

In the case of rare-earth orthoferrites, magnetic properties are affected by structural distortions and the interaction of Nd^{3+} and Fe^{3+} magnetic sublattices. It was also proposed that there might be a deficiency of oxygen ions in the lattice which pose as favourable sites for incorporation of excess Fe^{3+} ions resulting in an expansion of lattice and structural distortion of the system. Hence, it can be concluded that there might be an incorporation of Fe^{3+} ions in the vacant sites exhibiting strong ferromagnetic (Fe–O–Fe) interactions over the weak AFM interactions at higher temperature [24].

The results obtained indicate that the materials have a very high coercivity compared to those already known. These materials can be classified as hard magnetic according to the magnetization curve. This property in $NdFeO_3$ can be used in recording media and magnetic data storage applications. Therefore, the use of the Pechini method or heterogeneous precipitation methods with annealing at 1300 °C allows obtaining $NdFeO_3$ with higher magnetic properties than already known composites and widely used $LaFeO_3$ (Table 4).

IV. Conclusions

Phase equilibria were studied in the Nd_2O_3–Fe_2O_3 system at 1300 and 1400 °C. It has been established that solid state interactions between two oxides resulted in the formation of phases: $Nd(OH)_3$ labelled as A-Nd_2O_3, $NdFeO_3$ and Fe_2O_3. In the system Nd_2O_3–Fe_2O_3 at 1300 and 1400 °C, the ordered phase of perovskite type with rhombic distortion was revealed with composition corresponding to 51 mol% Nd_2O_3 – 49 mol% Fe_2O_3. Nanocomposites based on the perovskite phase ($NdFeO_3$) were obtained by the Pechini method and heterogeneous precipitation from nitrate solutions. Nanopowders are single-phase with a perovskite structure. The synthesized materials fully correspond to the $NdFeO_3$ phase both from the point of view of chemical analysis and from the point of view of diffraction. By using the Pechini method more agglomerated particles can be obtained, leading to a diffraction pattern for a polycrystalline material. At the same time, synthesis by heterogeneous precipitation allows for obtaining more homogeneous less agglomerated monocrystalline particles. The studied $NdFeO_3$ samples exhibited ferromagnetic behaviour at 1300 °C. The coercivity of the $NdFeO_3$(I) (1300 °C) and $NdFeO_3$(II) (heat-treated at 1300 °C) were 192 and 205 kA/m, respectively, and corresponding saturation magnetization were 0.8 and 0.81 kA/m, respectively.

Acknowledgements: We acknowledge the financial support of the European Commission through the project H2020-MSCA-RISE 2020 MELON (Grant No. 872631). The authors would like to acknowledge the access to the equipment of "Servicio General de Apoyo a la Investigación (SAI), Universidad de Zaragoza".

Table 4. Comparison of the $NdFeO_3$ magnetic properties with La_2O_3 and $LaFeO_3$

Composition	Methods of synthesis	*M* [emu/g]	Coercivity [kA/m]	Ref.
La_2O_3	Decompaction of polymer	0.03	-	[21]
Nd_2O_3	-	100	-	[22]
$LaFeO_3$ (I) (1300 °C)	Pechini method	0.2	40	[23]
$LaFeO_3$ (II) (1300 °C)	Heterogeneous precipitation	0.15	32	[23]
$NdFeO_3$ (I) (1300 °C)	Pechini method	0.8	192	Present work
$NdFeO_3$ (II) (1300 °C)	Heterogeneous precipitation	0.81	205	Present work
$NdFeO_3$	Single crystal	0.521	62	[24]
Fe_3O_4	Decomposition of $FeCl_3 \cdot 6H_2O$, NaAc	20	62	[25]

References

1. X. Gao, Y. Ji, M. Wang, Q. Liang, "Effect of Ba substitution on structure, magnetic properties and microwave properties of $NdFeO_3$", *Mater. Today Commun.*, **38** (2024) 108264.
2. P. Yadav, A. Pandey, B. Khan, R. Biswal, A. Fahad, P. Kumar, M. K. Singh, "Detailed investigation on structural, optical, dielectric and magneto-dielectric properties with enhanced magneto-impedance characteristic of $NdFeO_3$ nanoparticles", *Mater. Chem. Phys*., **309** (2023) 128424.
3. Z. Zhou, L. Guo, H. Yang, Q. Liu, F. Ye, "Hydrothermal synthesis and magnetic properties of multiferroic rare-earth orthoferrites", *J. Alloys Compd.*, **583** (2014) 21–31.
4. Z.-Q. Wang, Y.-S. Lan, Z.-Y. Zeng, X.-R. Chen, Q.-F. Chen, "Magnetic structures and optical properties of rare-earth orthoferrites $RFeO_3$ (R = Ho, Er, Tm and Lu)", *Solid State Commun.*, **288** (2019) 10–17.
5. A. Oliveira, M.L. Hneda, L.E. Fernandez-Outon, E.M. Barros de Sousa, J.D. Ardisson, "Synthesis and characterization of nanocomposites based on rare-earth orthoferrites and iron oxides for magnetic hyperthermia applications", *Ceram. Int*., **45** [14] (2019) 17920–17929.
6. C.L. Li, S.S. Zheng, G.O. Barasa, Y.F. Zhao, L. Wang, C.L. Wang, Y. Lu, Y. Qiu, J.B. Cheng, Y.S. Luo, "A comparative study on magnetic behaviors and magnetocaloric effect in heavy rare-earth antiferromagnetic orthoferrites $RFeO_3$ (R = Dy, Ho and Er)", *Ceram. Int*., **47** [24] (2021) 35160–35169.
7. X. Niu, H. Li, G. Liu, "Preparation, characterization and photocatalytic properties of $REFeO_3$ (RE = Sm, Eu, Gd)", *J. Mol. Catal. A: Chem.*, **232** (2005) 89–93.
8. J. Shankera, G. Narsinga Raob, K. Venkataramanaa, D. Suresh Babu, "Investigation of structural and electrical properties of $NdFeO_3$ perovskite nanocrystalline", *Phys. Lett. A*, **382** (2018) 2974–2977.
9. A. Hosakote Shankara, J. Samuel Prabagar, T. Tenzin, S. Yadav, K. Mallikarjunappa, A. Kumar, H. Puttaiah Shivaraju, "Facile synthesis of $NdFeO_3$ perovskite for photocatalytic degradation of organic dye and antibiotic", *Mater. Today Proceed*., **75** (2023) 15–23.
10. M. Nakhaei, D. Sanavi Khoshnoud, "Influence of particle size and lattice distortion on magnetic and dielectric properties of $NdFeO_3$ orthoferrite", *Physica B: Condensed Matter*, **553** (2019) 53–58.
11. Y. Khreif, M. Omari, S. Makhloufi, "Synthesis and catalytic properties of Ni-doped $NdFeO_3$", *Inorg. Chim. Acta*, **566** (2024) 122028.
12. X. Yang, S. Al Barwani, M. Alhabradi, M. Alruwaili, S. Saremi-Yarahmadi, T. Clarkson, A. Roy, K. Shanks, H. Chang, A. Ali Tahir, "Synthesis, characterization, and photocatalytic hydrogen evolution performance of neodymium iron composites: Influence of annealing temperature", *Inorg. Chem. Commun*., **158** (2023) 111592.
13. J. Shanker, M. Buchi Suresh, D. Suresh Babu, "Synthesis, characterization and electrical properties of $NdXO_3$ (X = Cr, Fe) Nanoparticles", *Mater. Today Proceed*., **3** (2016) 2091–2100.
14. S. Ahmad Mira, M. Ikrama, K. Asokan, "Structural, optical and dielectric properties of Ni substituted $NdFeO_3$", *Optik*, **125** (2014) 6903–6908.
15. E. Hadi Sujiono, V. Zharvan, M. Muchtar, S. Ade Poetra, A. Manab Idris, M. Yusriadi Dahlan, "Synthesis of ytterbium-doped neodymium ferrite oxide using solid-state reaction method and its characterization", *Mater. Today Proceed*., **44** (2021) 3323–3326.
16. X.-B. Lia, C. Gaoa, S. Suna, L.-L. Huanga, H. Zhoua, B.-X. Wua, L.-H. Zhengb, X.-F. Kanga, Y.-X. Zhaoa, F.-P. Wanga, J.-B. Zhang, "Ethanolamine gas sensors based on $NdFeO_3$ modified hexagonal pyramid shaped ZnO nanocrystals", *Ceram. Int*., **50** (2024) 26311–26324.
17. L.K. Jakobsson, G. Tranell, I.-H. Jung, "Experimental investigation and thermodynamic modeling of the B_2O_3-FeO-Fe_2O_3-Nd_2O_3 system for recycling of NdFeB magnet scrap", *Metal. Mater. Trans. B*, **48** (2017) 60–72.
18. N. Kimizuka, A. Yamamoto, H. Ohashi, T. Sugihara, T. Sekines, "The stability of the phases in the LnO-FeO-Fe_2O_3 systems which are stable at elevated temperatures (Ln: lanthanide elements and Y)", *J. Solid State Chem.*, **49** [1] (1983) 65–76.
19. S.C. Parida, S. Dash, Z. Singh, R. Prasad, K.T. Jacob, V. Venugopal, "Thermodynamic studies on $NdFeO_3$(s)", *J. Solid State Chem*., **164** [1] (2002) 34–41.
20. T. Katsura, T. Sekine, K. Kitayama, T. Sugihara, N. Kimizuka, "Thermodynamic properties of Fe-lanthanoid-O compounds at high temperatures", *J. Solid State Chem*., **23** [1] (1978) 43–57.
21. Z. Razmara, "Lanthanum(III) complex as ferromagnetic supraprecursor for preparation of La_2O_3 nanoparticles by thermal decomposition method", *Res. Chem. Intermed*., **45** (2019) 2887–2901.
22. G. Sala, M.B. Stone, B.K. Rai, A.F. May, C.R. Dela Cruz, H. Suriya Arachchige, G. Ehlers, V.R. Fanelli, V.O. Garlea, M.D. Lumsden, D. Mandrus, A.D. Christianson, "Physical properties of the trigonal binary compound Nd_2O_3", *Phys. Rev. Mater.*, **2** (2018) 114407.
23. O.V. Chudinovych, D.V. Vedel, O.O. Stasyuk, T.V. Tomila, M.H. Aguirre, "Production, structure and magnetic properties of nanocomposites based on the perovskite phase $LaFeO_3$", *Solid State Sci*., **157** (2024) 107699.
24. T. Shalini, P. Vijayakumar, J. Kumar, "Studies on structural and magnetic properties of $NdFeO_3$ single crystals grown by optical floating zone technique", *Bull. Mater. Sci*., **43** (2020) 285.
25. M.D. Nguyen, H.-V. Tran, S. Xu, T. Randall Lee, "Fe_3O_4 nanoparticles: Structures, synthesis, magnetic properties, surface functionalization, and emerging applications", *Appl. Sci.*, **11** [23] (2021) 11301.